A structural view of Pd model catalysts : high-pressure surface X-Ray diffraction

Rijn, R. van

Chapter 4

Spontaneous reaction oscillations on Pd(100): a new role for steps in catalysis

Atomic steps at the surface of a catalyst play an important role in heterogeneous catalysis, for example as special sites with increased catalytic activity. Under the influence of the reactants, entirely new structures may form at the catalyst surface under reaction conditions. These may dramatically influence the reaction, by poisoning it or by rather acting as the catalytically active phase. For example, thin metal oxide films have been identified to be highly active structures that form spontaneously on metal surfaces during the catalytic oxidation of carbon monoxide. Here we present operando surface x-ray diffraction experiments on a palladium surface during this reaction, which reveal that a high density of steps strongly alters the stability of the thin, catalytically active palladium oxide film. We show that this new stabilizing and destabilizing role of steps is at the heart of the well-known reaction rate oscillations during CO oxidation at atmospheric pressure.

Published as: *A new role for steps in catalysis and reaction oscillations*,
B. L. M. Hendriksen, M. D. Ackermann, R. van Rijn, D. Stoltz, I. Popa, O. Balmes, A. Resta, D. Wermeille, R. Felici, S. Ferrer, and J. W. M. Frenken,
Nature Chemistry **2**, 730-734 (2010).

4.1 Introduction

Atomic steps on catalyst surfaces are often considered as special, active sites for heterogeneous catalytic reactions [84]. Due to their reduced coordination, step sites can offer enhanced binding of reactant molecules [12, 85, 86] and exhibit enhanced activity for bond breaking [87–90]. Catalytic nanoparticles contain a high density of steps and the steps may dominate their activity. Steps also play a key role in many other surface processes, for example as the natural locations for crystal growth and erosion and as the source for mobile surface adatoms. In this chapter, we show that steps on surfaces may play a role in catalysis not only by serving as active sites, but also by changing the stability of the catalytically active phase.

Recent experiments and theory show that oxides form on the surface of precious metal catalysts such as Ru, Pt, Pd and Rh during oxidation catalysis at atmospheric pressure under oxygen-rich conditions [14, 23, 67, 91, 92]. Experiments performed under these conditions using operando techniques, which simultaneously provide information on the state of the catalyst and on the reaction kinetics, indicate that these oxides are catalytically more active than the bare metal surfaces [23, 91], although this is still the subject of ongoing debate [73]. The reason for the formation of the oxides is simply that at high oxygen pressures it is thermodynamically more favourable to incorporate oxygen atoms in the surface in oxygen-rich phases (oxides) than in the low-coverage chemisorption structures typical for low oxygen pressures.

Whether a catalyst operating in an oxidizing mixture of reactants prefers a mere chemisorption structure or an oxide [70, 92] depends on the partial pressures of the reactants. The transition of the catalyst surface from the metal phase to the oxide phase dramatically changes the catalytic reaction mechanism. Whereas on the metal surface both reactants first adsorb and then react to form the product (Langmuir-Hinshelwood mechanism), the more active oxidized surface serves as an intermediate product from which oxygen atoms are easily extracted by the other reactant (for example CO) after which the resulting oxygen vacancies are refilled with oxygen from the gas phase. This is similar to the Mars-Van Krevelen mechanism, in which gas molecules react with the lattice oxygen from the metal oxide to form the product while the redox process is completed by oxygen that diffuses through the oxide to fill up the oxygen vacancies that are caused by this reaction [10].

Previously we found that reaction rate oscillations can occur during CO oxidation under conditions where both the oxide and the metal phase can exist [51, 93]. Spontaneous and self-sustained oscillations in the rate of CO oxidation have been extensively studied both at low pressures (e.g. 10^{-6} mbar) and at atmospheric pressure [94, 95]. The low-pressure oscillations are due to atomic-scale restructuring of the surface of a catalyst (e.g. Pt or Pd) or the formation of a subsurface oxygen layer, as was shown beautifully in the work of G. Ertl et al [94]. By contrast, our earlier in situ scanning tunneling microscopy studies show that at atmospheric pressure the oscillations in the reaction rate are due to the spontaneous, periodic switching from a low-activity metal surface to a high-activity oxide surface [51, 93]. In this chapter we show that there is an important influence of the step density (roughness) on the stability of the metal and oxide phases of the catalyst's surface and that the steps thereby regulate the self-sustained reaction oscillations during CO oxidation on Pd(100) at atmospheric pressure.

4.2 Results

Figure 4.1 shows that the CO_2 production rate and the CO pressure inside a flow reactor spontaneously oscillated under steady state conditions and a constant feed of CO and O_2. The CO pressure oscillated in anti-phase with the CO_2 pressure as a result of the varying CO consumption in the reaction, which for the high rate is mass transfer limited [93]. Figure 4.1 shows surface x-ray diffraction (SXRD) data of the (h, k, l) = (1, 0, 2) diffraction peak of Pd(100) during oscillating CO oxidation at 447 K and $P_{CO} = 25$ mbar and $P_{O_2} = 500$ mbar in a 17 ml flow cell. The details of the experiment are given in the Methods section and the Supplementary Information. Movies are available online that show the oscillatory variations in the SXRD signals and the partial pressures of the reactant and product gasses (Supplementary Movie S1 and S2 of [72]).

In the low-reaction-rate phase ($P_{CO_2} = 2$ mbar) there was high intensity at the (h, k, l) = (1, 0, 2) diffraction peak, which shows that the surface was metallic. The inverse value of the full width of the diffraction peak at half the maximum intensity, $\mathrm{FWHM}^{-1}_{\mathrm{metal}}$, increased with time during this part of each oscillation. In the metal phase the $\mathrm{FWHM}^{-1}_{\mathrm{metal}}$ is a direct measure of the smoothness of the surfaces, in terms of the average terrace width, or, equivalently, the inverse of the step density [96]. The increase in $\mathrm{FWHM}^{-1}_{\mathrm{metal}}$ shows that the surface smoothened

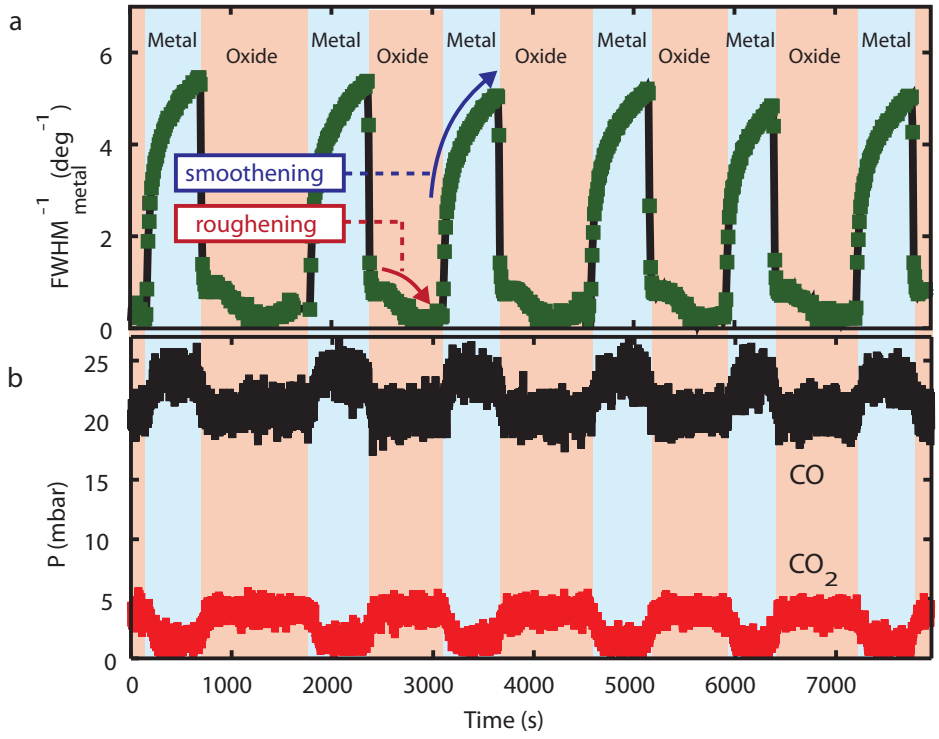

Figure 4.1: Spontaneous oscillations in the CO oxidation rate on Pd(100) as measured by SXRD and mass spectrometry. Measurements were performed at a temperature of 447 K in a constant flow of a CO/O_2/Ar gas mixture with an oxygen pressure of 500 mbar, an argon pressure of 675 mbar and a CO pressure of 25 mbar flowing at 50 ml_n min^{-1}. **a)** The $FWHM^{-1}_{metal}$ (inversely proportional to the step density and a measure of the smoothness of the surface) of the diffraction peak at (h, k, l) = (1, 0, 2). **b)** The partial pressure in the reactor of CO and CO_2 pressures as measured by mass spectrometry. At high CO partial pressures P_{CO}, the diffraction pattern shows that the surface structure is close to a bulk-like truncation of the Pd crystal (the reaction kinetics indicate that this metal surface is covered by a mixture of O atoms and CO molecules). At low P_{CO}, new diffraction peaks are found that correspond to a thin PdO(101) layer (e.g. (h, k, l) = (0.8, 0.4, 0.73) see Fig. 4.4). The colors indicate whether the SXRD intensities identify the Pd(100) surface to have a metal structure (light blue) or to be covered by a thin oxide film (light red).

by reducing its step density until the transition to the high-reaction-rate state occurred ($P_{CO_2} = 4.5$ mbar) and the Pd(100) (1, 0, 2) diffraction peak practically disappeared.

After the transition we observed a new diffraction peak at (h, k, l) = (0.8, 0.4, 0.73) (Fig. 4.4, Movie S2 of [72])), which we have determined to correspond to the presence of a 1.9 ± 0.5 nm thick PdO(001) film, similar to what has been found for Pd(100) in pure oxygen [49]. Additional, high-speed SXRD measurements show that this oxidation starts with the abrupt appearance of an ultrathin surface oxide with the well-known $(\sqrt{5} \times \sqrt{5})$R27° periodicity [49], which is replaced after typically 5 seconds by the epitaxial, bulk-like PdO film. The diffracted PdO intensity increased during ~ 7 seconds, which probably signifies the lateral closing of the bulk like PdO layer.

After this ~ 7 s period, the oxide layer thickness exhibits a power-law growth ($L \propto t^p$) with an exponent of $p = 0.28$ [97]. The transition to the high reaction rate coincided with the introduction of the $(\sqrt{5} \times \sqrt{5})$R27° structure and remained unchanged as the PdO film formed. In the oxide phase the $\mathrm{FWHM}_{\mathrm{metal}}^{-1}$ of the (low) intensity at (1, 0, 2) that remained is a measure of the smoothness of the interface between the metal Pd(100) substrate and the PdO(001) film covering it. The fact that the $\mathrm{FWHM}_{\mathrm{metal}}^{-1}$ decreased with time shows that the interface became rougher. The evolution of the PdO(101) (h, k, l) = (0.8, 0.4, 0.73) diffraction peak (that is, $\mathrm{FWHM}_{\mathrm{oxide}}^{-1}$) is shown in Fig. 4.4 and movie S2 in ref. [72].

The roughening in the oxide phase and the smoothing behaviour in the metal phase observed with SXRD are consistent with our high pressure scanning tunneling microscopy observations [93] (see Supplementary Information). Our interpretation is that during the Mars-Van Krevelen redox reaction on the oxide a small fraction of the metal atoms in the oxide becomes sufficiently strongly undercoordinated with oxygen to become mobile and diffuse out of their original positions until they are re-oxidized and immobilized on top of the oxide [14, 91]. The lack of mobility of the oxide at the low operation temperature prevents the resulting roughness from decaying before further roughness is added by the same process. As a result, roughness gradually accumulates, approximately linearly with the total amount of produced CO_2. In the metallic phase we observe high surface mobility and the reaction does not cause further roughening, so that the surface roughness decays with time.

When we consider the timescales of the stages of an oscillation cycle we see that the metal-to-oxide and oxide-to-metal transitions are practically 'instanta-

neous'. The ultrathin surface oxide appears within 2 s and the PdO disappears exponentially with a typical timescale of 6 s. However, the smoothening of the metal and roughening of the oxide are slower processes. Therefore we propose that the variation of the roughness, i.e. the step density, induces both transitions and thereby regulates the oscillations to have periods on the order of 1000 s.

To prove that indeed the roughness is responsible for inducing the phase transition we performed separate SXRD experiments in a 2-liter batch reactor that we pre-filled each time with a specific mixture of oxygen and CO. This mode of operation does not lead to spontaneous self-sustained oscillations, which enables us to separate cause and effect of the oscillations. These experiments allow us to derive the stability diagram of Fig. 4.2, which shows the minimum partial pressure of CO, at which the metal is stable against oxidation, as a function of the surface roughness, $\mathrm{FWHM_{metal}}$. In order to use the roughness of the metal surface as a control parameter, we "prepared" the surface in each experiment by keeping it in the metal phase for a different amount of time, a longer time resulting in a smoother surface (lower $\mathrm{FWHM_{metal}}$). In practice, this was done by starting each batch experiment at a different partial pressure of CO, at a fixed initial O_2 pressure. The details of this procedure are given in the Supplementary Information.

In each experiment, the two reactants were slowly converted to CO_2, thereby reducing the ratio between P_{CO} and P_{O_2}. During this stage the initially rough metal surface slowly smoothened as we determined from the decreasing FWHM of the (1, 0, 0.2) diffraction peak, which is close to equivalent to the (1, 0, 2) peak of Fig. 4.1. The smoothening continued until the metal-to-oxide transition took place, which was accompanied by a tenfold increase in the CO_2 production rate and the appearance of the diffraction peak at (0.8, 0.4, 0.73) of the PdO(101) film. We performed this procedure four times, each time for a different initial value of P_{CO}. This resulted in the four curves of P_{CO} versus $\mathrm{FWHM_{metal}}$ in Fig. 4.2. The lowest CO pressure in each curve, P^*_{CO} , indicates the conditions at which the metal-to-oxide transition took place. Figure 4.2 fully confirms our suspicion that roughness has a dramatic influence on the stability of the metal with respect to oxidation. The critical CO pressure,P^*_{CO}, shows a one-to-one correspondence with the step density. A significantly more oxidizing CO/O_2 mixture is required to oxidise a rough surface than a smooth surface. From a kinetic point of view this is unexpected since steps actually facilitate oxidation [98], but we argue below that it is a thermodynamic effect.

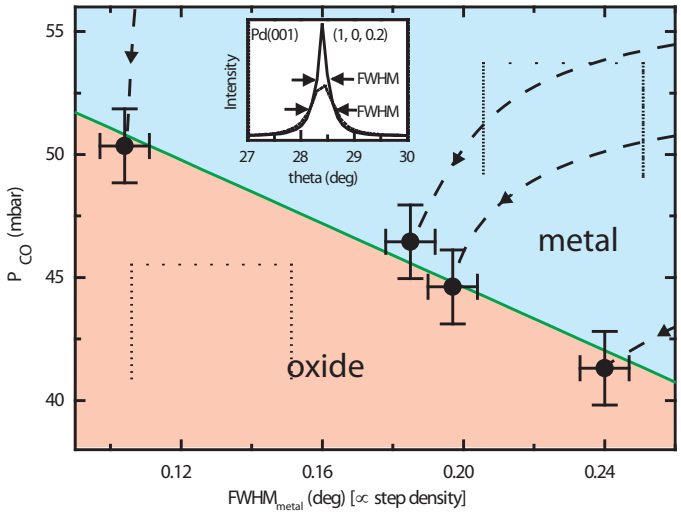

Figure 4.2: Stability diagram of the Pd(100) surface measured with surface x-ray diffraction. Measurements were performed at a temperature of 460 K in a CO/O_2 gas mixture with a fixed oxygen partial pressure of P_{O_2} = 0.48 bar in a batch reactor. The parameter along the horizontal axis of the main figure is the $FWHM_{metal}$ of the diffraction peak on the metal surface with reciprocal coordinates (h, k, l) = (1, 0, 0.2) immediately prior to the metal-to-oxide transition. This peak width is a sensitive measure of the density of steps on the metal surface. The trajectories of ($FWHM_{metal}$,P_{CO} approaching the metal-oxide transition are indicated by the four dashed curves. The error margins reflect the maximum variations observed in the peak width and the CO pressure at the transition. The inset shows two diffraction peaks on a trajectory at different $FWHM_{metal}$.

4.3 Discussion

Thermodynamically, the first-order metal-oxide transition of a smooth, step-free surface takes place when the free energies of the two competing structures, namely the metal surface with a chemisorbed layer of reactants and the oxide surface, are equal. The presence of steps shifts this balance because steps on both phases cost different amounts of (free) energy. This shift can go either way, but there are two arguments why steps could work in favour of the metal phase and make it stable down to a lower CO pressure (P^*_{CO}). First, on many metal surfaces CO molecules adsorb significantly more strongly at steps than on terraces [12, 85, 86]. For a metal surface in contact with CO, this reduces the effective step free energy

and under special circumstances can even lead to the spontaneous formation of steps [99]. We anticipate that this enhanced bonding effect is stronger for CO molecules than for O atoms adsorbed at steps on Pd(100) [100]. We propose that this reduction of the effective step free energy by CO adsorption stabilizes a rough metal phase with respect to a rough oxide phase. Secondly, steps make the metal surface a bad template for the PdO(101) structure, since they necessarily lead to dislocations in the oxide. The effect of the step density on the metal-oxide transition is reminiscent of the role of steps in the phase transition from the 7×7 surface reconstruction to the 1×1 phase on Si(111), for which the transition temperature depends on step density [101].

The combination of all experimental observations leads to a simple scenario for the self-sustained reaction oscillations (Fig. 4.3).
Each cycle **(A)**→**(B)**→**(C)**→**(D)** contains the following four stages.

1. **(A)**→**(B)**: comprises a decrease in metal surface roughness. The cycle starts with a rough metal surface. The reaction follows the Langmuir-Hinshelwood (gas adsorption and reaction) mechanism, resulting in a low reaction rate R_{metal}. In the metal phase the surface smoothens, which shifts the conditions towards the metal-oxide phase transition (P^*_{CO} increasing towards P_{CO}).

2. **(B)**→**(C)**: represents the metal-to-oxide transition. When the step density decreases enough and $P^*_{\mathrm{CO}} = P_{\mathrm{CO}}$, then the surface oxidizes. The reaction rate changes abruptly to the Mars-van-Krevelen (oxide reduction and re-oxidation) mechanism with the high reaction rate R_{oxide}. Now that more CO is being consumed, P_{CO} is reduced in the vicinity of the active surface by an amount ΔP_{CO}, which further stabilizes the oxide. Note, that in this description we do not distinguish between the observed oxide structures ($(\sqrt{5} \times \sqrt{5})$ and PdO), as the reaction rate is equally high for both of them.

3. **(C)**→**(D)**: comprises an increase in oxide roughness. The Mars-Van Krevelen reaction mechanism leads to a slow build-up of surface roughness. This, in turn, reduces P^*_{CO} towards P_{CO} towards.

4. **(D)**→**(A)**: comprises the oxide-to-metal transition. When the oxide has become sufficiently rough that $P^*_{\mathrm{CO}} = P_{\mathrm{CO}}$, the system switches back to a (rough) metal surface. The reaction changes abruptly to the Langmuir-Hinshelwood mechanism again, reducing the reaction rate to R_{metal}, thus

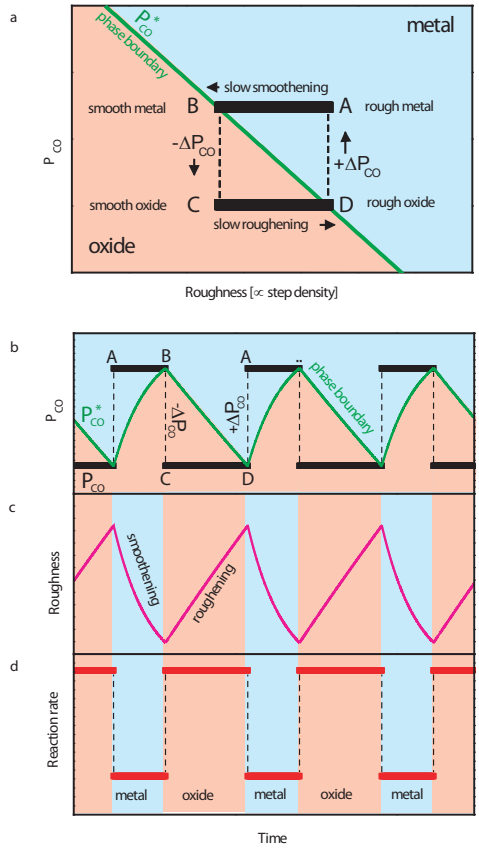

Figure 4.3: Generic model for the reaction rate oscillations. Each cycle takes the surface through stages **(A)** rough metal, **(B)** smooth metal, **(C)** smooth oxide, and **(D)** rough oxide, after which the next cycle starts again at **(A)**. **a)** The metal-oxide stability diagram (cf. Fig. 4.2), in which the phase boundary is determined by the roughness and the CO partial pressure, P^*_{CO}. Per cycle the surface crosses this boundary twice (at **B** and at **D**). **b-d)** The variations in roughness, P_{CO}, and reaction rate (P_{CO_2}) during three complete cycles. In the oxide phase, the surface becomes progressively rough, whereas it smoothens in the metal phase **b)**. As can be read off from **a)**, these variations in roughness introduce corresponding variations in the P^*_{CO} value of the metal-oxide transition, which are indicated by the green line in **b)**. At points **B** and **D** in the cycle, this critical P^*_{CO} value becomes equal to the actual CO pressure P_{CO} (black lines in **b)**) and the phase transition takes place. Since the reaction rate on the oxide is higher than that on the metal **d)**, the CO pressure in the reactor switches up or down by ΔP_{CO} every time the surface is reduced or oxidized (black lines in **b)**).

increasing P_{CO} by ΔP_{CO} and further stabilizing the metal phase. This restores the starting conditions and closes the cycle.

The period of the oscillation is determined by the magnitude of ΔP_{CO} and by the smoothening and roughening rates in the metal and oxide phases.

With the exception of the effect of the oxide roughness on the oxide-to-metal transition all characteristics of this scenario are based on experimental observations. These characteristics include increasing and decreasing oxide and metal roughness respectively; the dependence of P^*_{CO} on roughness; the different reaction mechanisms and rates; and the resulting changes in local P_{CO}.

We have also tested the scenario in a simple numerical calculation, in which we modelled the roughness evolution and the dependence of P^*_{CO} on roughness with first-order differential equations. The results of the calculation, under steady state conditions, are shown in Fig. 4.3 (for the details of this calculation see the Methods section and the Supplementary Information). Although the model is too crude to faithfully describe all details of the CO oxidation reaction on Pd(100), it fully captures the essence of the observed oscillations, such as the influence of P_{CO} on the oscillation period and on the ratio between the metal and oxide parts of the oscillations.

Our observations and interpretation of reaction oscillations are at variance with existing models for reaction oscillations during CO oxidation on Pt-group metals. We observed that the system oscillates between a metal surface with O and CO chemisorbed (low reaction rate) and the thin oxide layer (high reaction rate). The periodic transition between the metal and the oxide is caused by the formation and decay of roughness (steps). By contrast, at low pressures ($< 10^{-6}$ mbar) oscillations are caused by variations in the concentration of the chemisorbed reactants, periodically switching between two stable sates of Langmuir-Hinshelwood kinetics: a chemisorbed O-dominated (high reaction rate) and a CO-dominated metal surface (low reaction rate), coupled to adsorbate induced restructuring of the metal surface or the insertion of subsurface oxygen species [94]. At atmospheric pressures -the regime discussed here- oxides play a role and according to the widely accepted model proposed by Sales et al. the switching between chemisorbed O-dominated (high reaction rate) and CO-dominated (low reaction rate) metal surface is caused by the slow formation of a catalytically inactive oxide [95, 102].

Based on our model and simple diffusion and reaction-rate considerations, we

predict that the oscillation period should be a strong function of temperature, with higher temperatures leading to much shorter periods. Vicinal surfaces, which have high step densities by themselves, are expected to oxidise at lower CO pressures compared to low-index surfaces. In addition, the period of the metal phase of an oscillation cycle on a vicinal surface should be short as the length over which atoms have to move to restore the initial (high) step density is short. Another important element is hidden in the design of the reactor and, in particular, in the flow resistance of the gas line between the CO pressure regulator and the reactor, since this resistance determines the strength ΔP_{CO} of the pressure variations. This quantity dictates how wide or narrow the window is of pressures for which the system will exhibit spontaneous reaction oscillations and it also has a direct influence on the oscillation period. This aspect may be responsible for the large variation in oscillation behaviour found for the same reaction systems between different instruments or different research groups [95].

Our scenario presents a new mechanism for oscillatory oxidation reactions at atmospheric pressure. It is not specific for Pd(100); we have observed similar oscillations in CO oxidation on several other Pd and Pt surfaces [103]. Equivalent oscillation mechanisms, again involving the role of steps, may be at play in other catalytic reaction systems, e.g. other oxidation reactions or reactions involving the formation of other surface species, such as carbides, sulphides or nitrides.

The new role identified here for roughness in heterogeneous catalysis may serve as a specific target for future catalyst design; think of new structural promoters that inhibit the formation of steps or enhance surface mobility and thus increase the decay rate of the roughness.

4.4 Methods and supplementary information

The surface x-ray diffraction (SXRD) experiments were performed at the ID03 beamline of the European Synchrotron Radiation Facility (ESRF) in two separate set-ups. One is a combined ultrahigh vacuum - high pressure SXRD chamber (10^{-10} mbar - 2 bar), which has a volume of ~ 2 l and was equipped with a 360°cylindrical beryllium window for entrance and exit of the x-rays [21]. The other set-up is a combined UHV-high pressure (10^{-9} mbar - 1.2 bar) flow reactor, which has a volume of 17 ml [74, 77]. The top part of the reactor is a beryllium dome allowing for entrance of the incident and exit of the diffracted x-ray beam.

The chambers were mounted on a z-axis diffractometer with the crystal surface in a horizontal plane. We have used a focused beam of monochromatic, 17 keV or 20 keV x-rays, impinging on the surface at a grazing angle of typically 1°.

High-pressure scanning tunneling microscopy (HP-STM) measurements were performed in a dedicated Reactor-STM, which combined preparation and characterization of the surface under ultrahigh vacuum conditions with STM experiments in an integrated flow-reactor cell (volume 0.4 ml) at temperatures up to 500 K and pressures up to 5 bar [104, 105].

All instruments are equipped with a gas manifold with pressure regulators and flow controllers, with which the pressure, composition and flow rate of high-purity mixtures of O_2 and CO could be prepared. In the experiments a quadrupole mass spectrometer was used for online analysis of the gas composition in the reactor. In all experiments a mechanically polished, (001) oriented, Pd crystal was used that was prepared in situ, under ultrahigh vacuum conditions. In each setup, the temperature of the Pd was measured with a thermocouple and regulated to within ΔT=2 K. Only in the batch reactor, the exothermic reaction led to a temperature increase higher than this, when the surface switched from metal to oxide, but all measurements combined in Fig. 4.2 were taken in the metal phase and were not affected by this.

In all experiments a mechanically polished, (001) oriented, Pd crystal was used that was prepared in situ, under ultrahigh vacuum conditions. Several cycles were necessary of a standard procedure, involving Ar^+ ion bombardment and annealing, in order to obtain a well-ordered Pd(100) surface with a low step density, as was verified with SXRD, low-energy electron diffraction and STM.

In the numerical model used to calculate the graphs shown in Fig. 4.3 each of the two phases of the surface, metal and oxide, is characterized by two rates, namely the reaction rate of CO oxidation and the rate of change of the surface roughness (see Supplementary Information). The condition for the surface to be either in the oxide or the metal phase was $P_{CO} < P^*_{CO}(\rho)$ for the oxide and $P_{CO} > P^*_{CO}(\rho)$ for the metal, with P_{CO} the CO pressure in the reactor near the surface and $P^*_{CO}(\rho)$ the critical CO pressure at which the transition takes place, which depends on the roughness ρ as $P^*_{CO}(\rho) = P^*_{CO}(0) - d\rho P^*_{CO}(0)$, where $P^*_{CO}(0)$ is the critical CO pressure for zero roughness, d is a positive constant and the normalized roughness is $0 \leq \rho < 1$. In the model the roughness increases in the oxide phase, proportional to the reaction rate. In the metal phase the roughness decays exponentially with time.

4.4.1 SXRD in flow cell: oscillations

After closing the reactor, a constant 50 $ml_n\ min^{-1}$ gas flow composed of 675 mbar Ar, 500 mbar O_2, and 25 mbar CO was admitted in the reactor. A direct leak from the reactor into the UHV allowed us to analyze the gas composition in the reactor. To obtain optimal time resolution for the SXRD ($\sim$ 1 s) the diffraction signal was recorded using the Maxipix 2D pixel detector [79, 106].

In two separate experiments two diffraction signals were recorded during the spontaneous oscillations: the Pd(100) (h, k, l) = (1, 0, 2) anti-Bragg position (Fig. 4.1) and the (h, k, l) =(0.8, 0.4, 0.73) position characteristic of the approximately 1.9 nm thick bulk-like PdO overlayer. Figure 4.4 shows the inverse FWHM of the oxide diffraction peak, $FWHM^{-1}_{oxide}$. In Fig. 4.4 one can clearly see the decrease of the domain size of the PdO overlayer, indicating the roughening of the layer. Peak widths $FWHM_{metal}$ and $FWHM_{oxide}$ were obtained from fitting a Lorentzian peak shape to the diffraction signals as shown in Movie S1 (1, 0, 2) and Movie S2 (0.8, 0.4, 0.73) of the supplementary material of [72].

Pd(100) does not reconstruct and therefore the correlation length of the x-ray diffraction, given by the inverse of the full width at half of the maximum intensity $FWHM^{-1}_{metal}$ of the (h, k, l) = (1, 0, 2) diffraction peak, is equivalent to the average terrace width (it is the same for the (h, k, l) = (1, 0, 0.2) peak used in the batch experiment described below). The presence of roughness (steps) reduces the average terrace width causing a broadening of the diffraction peak. Strain may also broaden the diffraction peaks, but based on the STM observations (see below) we conclude that roughness is dominating the $FWHM_{metal}$ values.

4.4.2 STM in flow cell: oscillations

To complement our SXRD data with real space microscopic information we show scanning tunneling microscopy data that were recorded on a Pd(100) surface inside a micro-flow reactor during oscillatory CO oxidation at a total pressure of 1.2 bar, a flow of 4 $ml_n\ min^{-1}$ and a temperature of 408 K. The combination of the mass spectrometry signals and the STM images are shown in Fig. 4.5. Figure 4.5a shows that the CO oxidation rate on Pd(100) in a constant reactant flow at atmospheric pressure spontaneously oscillates between two distinct levels, R_{oxide} and R_{metal}. The oscillations in the CO pressure in the reactor are in anti-phase with the variations in CO_2 production and are caused by the difference in CO

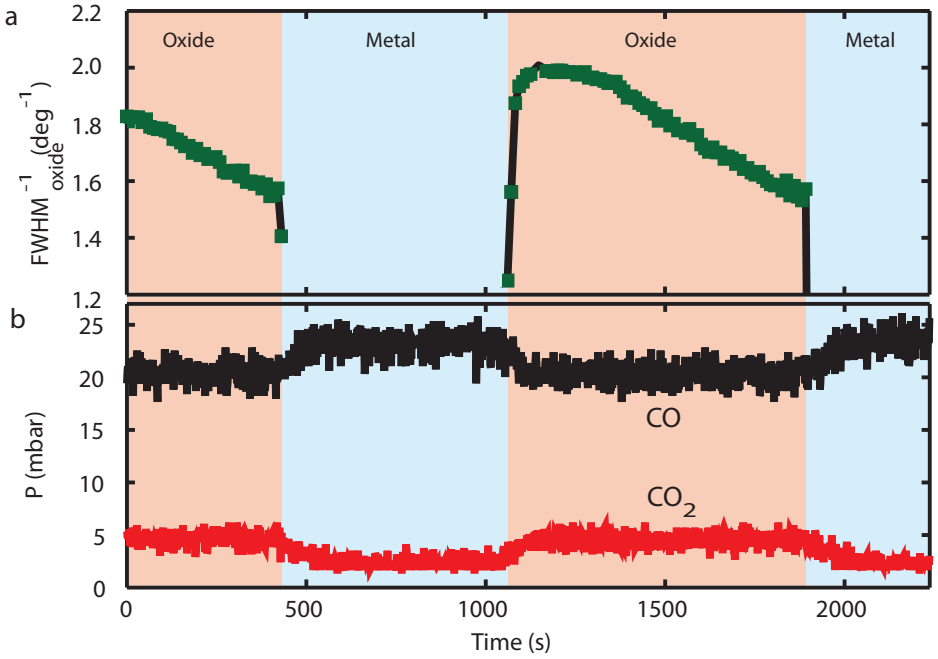

Figure 4.4: Oxide diffraction peak during oscillations in the CO oxidation rate on Pd(100). Measurements were performed at a temperature of 447 K in a $CO/O_2/Ar$ gas mixture with an O_2 pressure of 500 mbar, an Ar pressure of 675 mbar and a CO pressure of 25 mbar flowing at 50 ml_n min^{-1}. **a)** The $FWHM^{-1}_{oxide}$ (proportional to the domain size) of the PdO diffraction peak at (h, k, l) = (0.8, 0.4, 0.73). **b)** The partial CO and CO_2 pressures in the reactor as measured simultaneously by mass spectrometry.

consumption at the two reaction rates. Figure 4.5 shows STM images that were recorded during these self-sustained reaction oscillations. They were recorded in 100 s per image and therefore contain both spatial and temporal information of the topography. Scan lines of the images were synchronized with the mass spectrometry data along the horizontal time axis. In our earlier high-pressure STM studies we had already found that the oscillations are the periodic switching between the low-activity metal phase and the high-activity oxide and these changes in structure can be recognized also in Fig. 4.5 [51]. The metal phase is characterized by height variations of multiples of the step height of Pd(100) and step

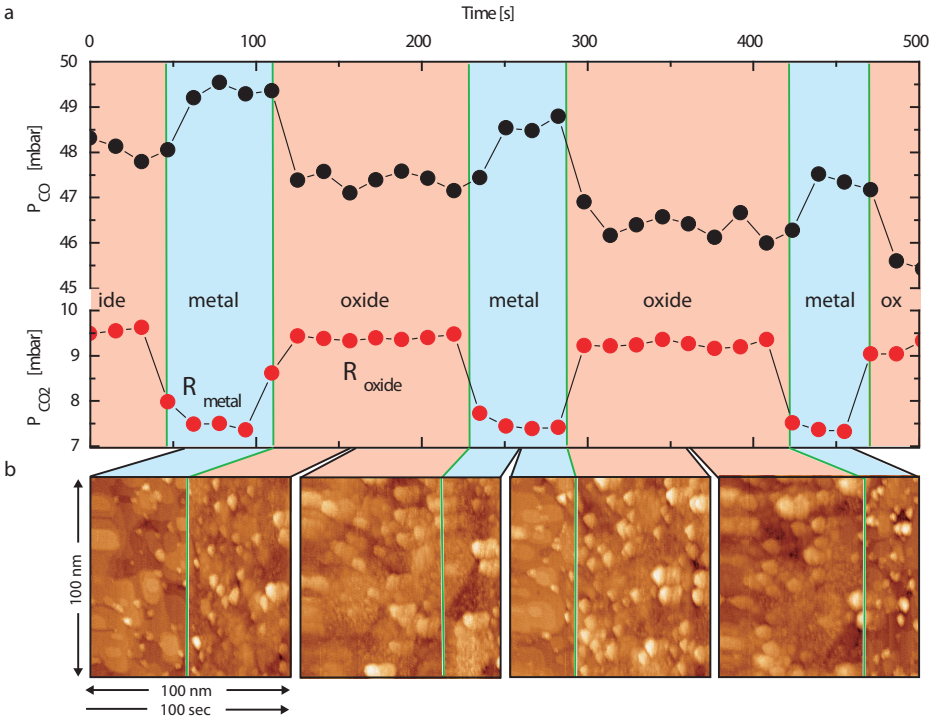

Figure 4.5: Scanning tunneling microscopy during oscillations in the CO oxidation rate on Pd(100). **a)** The reaction rate (P_{CO_2}) and the CO pressure (P_{CO}), observed in a flow reactor at a constant O_2 pressure of P_{O_2} 1.2 bar and a temperature of 408 K. **b)** The scanning tunneling microscopy images ($V_t = 100$ mV, $I_t = 0.2$ nA, image size: 100 nm$\times$100 nm, slow scan direction along the time axis) have been recorded simultaneously with the CO_2 and CO pressures and show that the oscillations are accompanied by the oxidation and reduction of the Pd surface. The metal phase exhibits characteristic terrace-and-step configurations with the well-defined step height of Pd(100), while the oxide is rougher and shows no such order.

and island structures are visible. The experiment started with a smooth Pd(100) surface with a typical initial step density of 0.03 step nm^{-1} measured in the fast scan direction. During the oscillations shown in Fig. 4.5 the step density on the metal varied from 0.2 step nm^{-1} to 0.1 step nm^{-1} determined along the fast scan direction. The oxide surface is dominated by roughness with no repeating height unit. From the changes both in the reaction rates and in the STM images we see that the metal-oxide and oxide-metal transitions take only a fraction of a second, while the period of the oscillations can be many minutes. The STM data illustrate the presence and the variations of roughness during the oscillations.

4.4.3 SXRD in batch reactor: pulse experiment

The four ($FWHM_{metal}$, P^*_{CO}) data points of the phase diagram of Fig. 4.2 were taken from Fig. 4.6, which in (a) shows the partial pressures of CO, O_2, and CO_2 in the reaction chamber during CO oxidation experiments at a temperature of 460 K. Figure 4.6 shows a series of rocking scans of the Pd(100) crystal truncation rod (surface diffraction peak) at (h, k, l) = (1, 0, 0.2) that had been recorded simultaneously. The reaction chamber was operated in batch mode, which means that we added CO at t_1, t_3, t_5, t_7 to restart the reaction, each time after all previously admitted CO had been converted to CO_2. By also adding O_2 we kept the oxygen pressure constant over the duration of the experiment. The reaction product CO2 gradually accumulated in the chamber. (Note that whenever we introduced gas to the chamber there were transients in all the mass spectrometer signals at $t = 10, 12, 56, 60, 98, 107, 140, 169$ min. These transients are related to our gas sampling and detection and not to the reaction kinetics.)

The experiment started at t_0 in 480 mbar O_2 and 230 mbar CO_2, left over from a previous reaction cycle. Under these conditions we observed a diffraction peak at (0.8, 0.4, 0.74), corresponding to palladium oxide, i.e. PdO(101) (Fig. 4.6). There was no intensity at the metal Pd(100) position (1, 0, 0.2). At $t = 10$ min. we added O_2 to the chamber through a leak valve to increase P_{O_2} to 500 mbar. At t_1 we added 52 mbar of CO to the chamber. The CO reacted with O_2 to the reaction product CO_2, as shown by the linear decrease of the CO and O_2 pressures and the increase in the CO_2 pressure in Fig. 4.6 for $t_1 < t < t_2$. Figure 4.6 shows that as soon as we introduced the CO at t_1 the Pd(100) diffraction peak appeared at (1, 0, 0.2). The PdO(101) peak had vanished completely. The CO pressure increase had induced the oxide-to-metal transition.

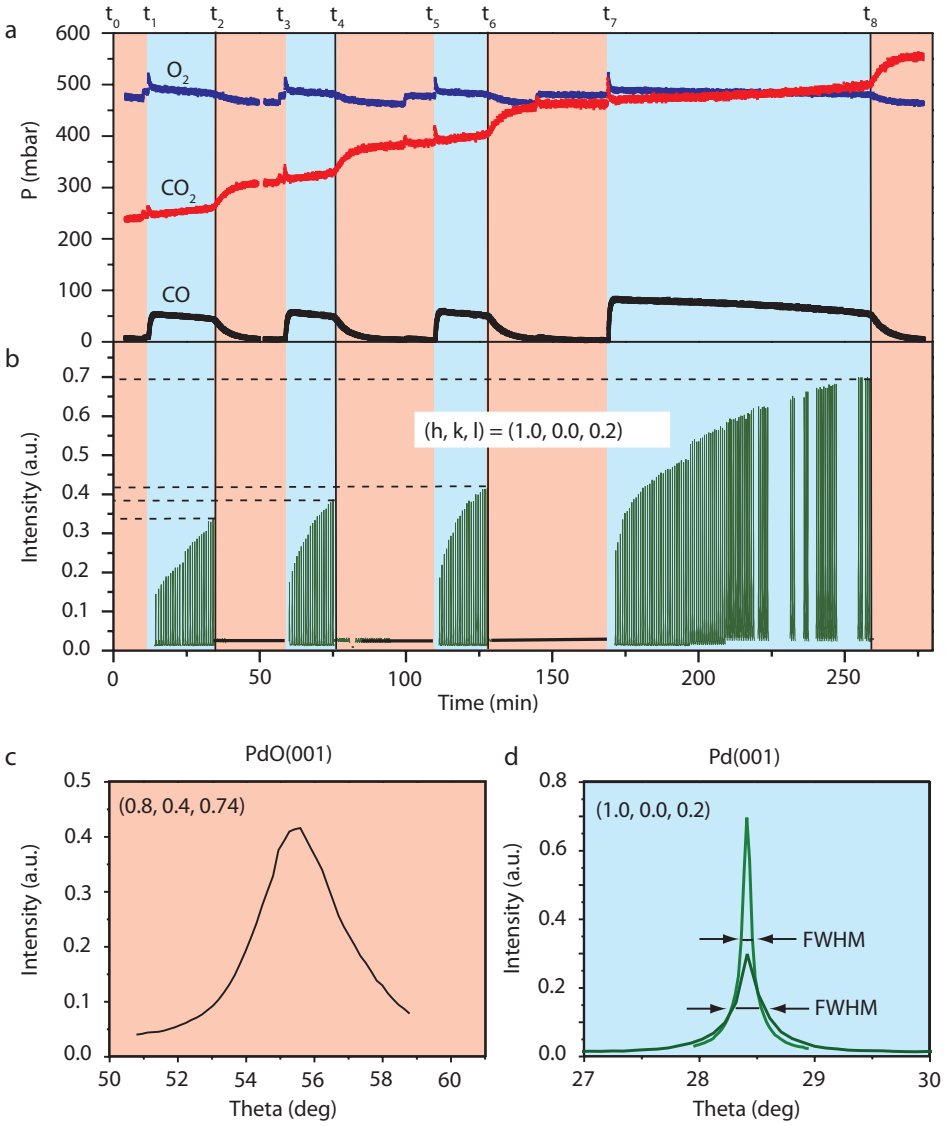

Figure 4.6: Cycles of spontaneous oxidation and forced reduction of the Pd(100) surface during CO oxidation at 460 K in a batch reactor. **a)** Partial pressures of the reactants CO and O_2 and the reaction product CO_2. **b)** Series of rocking scans of the Pd(100) surface diffraction peak at (h, k, l) = (1, 0, 0.2). **c)** Rocking scan of the PdO(001) peak of the oxidized palladium surface at (h, k, l) = (0.8, 0.4, 0.74). **d)** Individual rocking scan of the (1, 0, 0.2) crystal truncation rod of Pd(100) from the series in **(b)**.

In the metal phase the height of the Pd(100) peak increased with time. As the integrated intensity of the peak remained constant, the increase in height directly implies that the $FWHM_{metal}$ decreased. The $FWHM_{metal}$ of the Pd(100) diffraction peak is inversely proportional to the coherence length of the Pd surface structure, which is equivalent to the average terrace width. The $FWHM_{metal}$ is therefore a direct measure of the step density. The decrease of the $FWHM_{metal}$ with time reflects the slow smoothening of the Pd(100) surface by reduction of the step density. At t_2 the (1, 0, 0.2) diffraction peak spontaneously disappeared on a timescale of less than one second. Simultaneously, the reaction rate increased by a factor of 10. In this reaction cycle we recorded only the diffraction peak of Pd(100) at (1, 0, 0.2), but from other cycles we know that at t_2 the PdO(101) peak at (0.8, 0.4, 0.74) instantly reappeared, as shown in Fig. 4.6c. The spontaneous event observed at t_2 was the metal-oxide phase transition of the palladium surface. After all CO had been consumed we again added oxygen, followed by a 55 mbar CO pulse at t_3, which started the second cycle. At each new cycle we increased the amount of CO added, which increased the time needed for the reaction on the metal surface to reduce the CO pressure in the chamber by reaction to CO_2 to the critical CO pressure P^*_{CO}. This delayed the metal-to-oxide transition and therefore allowed the metal surface more time to smoothen. The combinations of the critical $FWHM_{metal}$ value of the (1, 0, 0.2) diffraction peak and the critical CO pressure at the metal oxide transitions at t_2, t_4, t_6, and t_8 define the metal-oxide phase boundary in Fig. 4.2. This experimental procedure used to determine the stability diagram ($FWHM_{metal}$, P^*_{CO}) did not allow us to perform a similar analysis of ($FWHM_{oxide}$, P^*_{CO}) for the oxide-to-metal transition.

4.4.4 Numerical model for reaction rate oscillations

In our model, each of the two phases of the surface, metal and oxide, is characterized by two rates, namely the reaction rate of CO oxidation and the rate of change of the surface roughness. These rates are summarized in Table 4.1. The reaction rate R_{metal} on the metal (Eq. (4.1)) corresponds to 'text-book' Langmuir-Hinshelwood kinetics in which O_2 adsorbs dissociatively and CO molecularly. The constants k_1 and k_2 are ratios of the rate constants for adsorption and desorption of O_2 and CO respectively. The reaction rate on the oxide (Eq. (4.3)) reflects our observation that R_{oxide} is proportional to the CO pressure and independent of P_{O_2} [104].

Table 4.1: Rate equations for the numerical model.

	Reaction rate		Rate of change in roughness	
Metal	$R_{\text{metal}} = \frac{\sqrt{k_1 P_{O_2}} k_2 P_{CO}}{\left(\sqrt{k_1 P_{O_2}} + k_2 P_{CO} + 1\right)^2}$	(4.1)	$\frac{d\rho}{dt} = -a\rho$	(4.2)
Oxide	$R_{\text{oxide}} = k_3 P_{CO}$	(4.3)	$\frac{d\rho}{dt} = b\,(1-\rho)\,R_{\text{oxide}}$	(4.4)

We express the roughness of the surface in a dimensionless parameter ρ, which can vary between 0 (completely smooth surface) and 1 (maximally rough surface). On the metal surface there are several competing diffusion mechanisms that reduce the step density, each with its own non-trivial scaling behaviour with time. In the SXRD experiments, however, we find that the net result is very well described by exponential decay of the roughness. In the model this is introduced by making the rate of roughness change proportional to $-\rho$ (Eq. (4.2)). On the oxide, roughness is observed as a 'by-product' of the reaction. For the oxide on Pt(110) we have measured by STM that roughness was produced approximately proportional to the amount of produced CO_2 [104]. For Pd(100) we have not been able to perform a similar analysis, but we nevertheless assume that the rate of reaction-induced roughening on the oxide is proportional to R_{oxide} (Eq. (4.4)). The extra factor $(1-\rho)$ in the oxide's roughening rate limits the roughness to the interval $[0;1)$. The constants and a and b in Eqs. (4.2) and (4.4) are both positive.

An important element in the model is the change $\pm\Delta P_{CO}$ in local CO pressure when the surface oxidizes or reduces. This change is directly proportional to the change in reaction rate

$$\Delta P_{CO} = c\,(R_{\text{oxide}} - R_{\text{metal}}) \tag{4.5}$$

where c is a positive constant. For oscillations under steady-state conditions R_{oxide} and R_{metal} are constant and so is ΔP_{CO}.

Finally and most importantly, we need to specify the relation between the CO pressure P^*_{CO} at which the metal-oxide phase transition takes place and the surface roughness ρ. As we have seen experimentally in Fig. 4.2 we can describe this by a linear relation

$$P^*_{CO}(\rho) = P^*_{CO}(0) - d\rho, \tag{4.6}$$

where d is a positive constant. When P_{CO} is higher than $P^*_{CO}(\rho)$, the surface is in the metallic phase with the reaction rate and roughness variation being prescribed

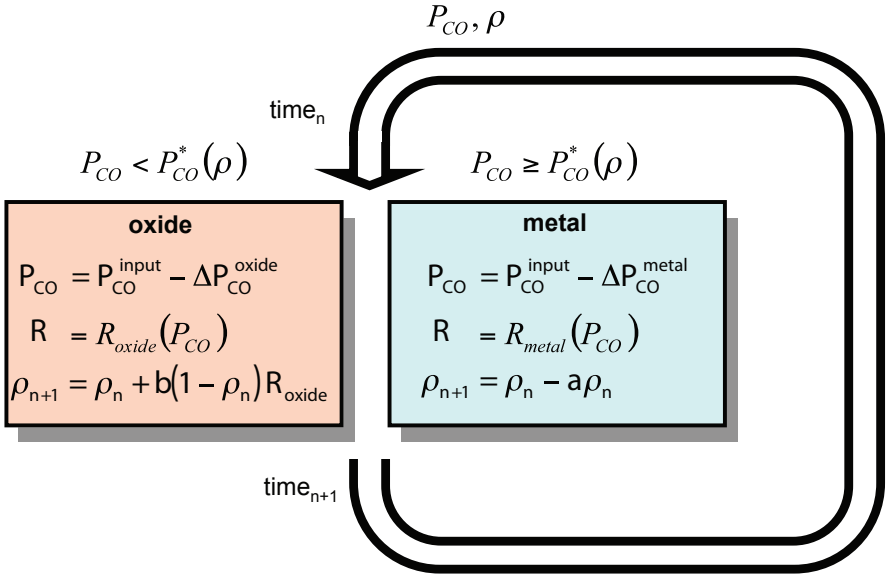

Figure 4.7: Scheme of the numerical model for self-sustained oscillations at constant oxygen pressure. At the beginning of each numerical time step the local CO pressure P_{CO} and the roughness ρ determine (through P^*_{CO}) whether the surface is in the metal phase or in the oxide phase. If the system is in the metal phase the local CO pressure is equal to $P_{CO} = P_{CO^{input}} - \Delta P_{CO}$, close to the partial pressure of CO in the supplied gas flow ($P_{CO^{input}}$), the reaction rate follows Eq. (4.1), and the roughness decreases from ρ_n to ρ_{n+1} according to Eq. (4.2). In the oxide phase the local CO pressure is reduced by $\Delta P_{CO} = \Delta P^{oxide}_{CO} - \Delta P^{metal}_{CO}$ as a result of the higher reaction rate. The reaction rate follows Eq. (4.3), and the reaction induced roughness increases at a rate proportional to the reaction rate, as given by Eq. (4.4).

by Eqs. (4.1) and (4.2). When it is below $P^*_{CO}(\rho)$, the surface is in the oxide phase and the rates are given by Eqs. (4.3) and (4.4).

Together, Eqs. (4.1) to (4.6) successfully describe the characteristics of the self-sustained oscillations experimentally observed under steady-state reaction conditions as well as the transient oscillations observed during slow ramps in the CO partial pressure. The numerical scheme, based on Eqs. (4.1) to (4.6), which we used to calculate the reaction rate oscillations of Fig. 4.3 is shown in Fig. 4.7.

Equations (4.2), (4.4) and (4.6) only use a single roughness parameter to describe the roughness of both the metal and the oxide. Accordingly the roughness

shows no discontinuity at the phase transition in Fig. 4.3. However, the density of Pd atoms in the oxide is different from the density in the metal. As a consequence, the formation of the oxide on an initially flat Pd(100) surface leads to approximately 20% of the oxidized surface being covered by islands of expelled (and subsequently oxidized) Pd. This introduces an abrupt increase in step density when the surface oxidises. When the surface is reduced again, we do not observe an equivalent, abrupt decrease in the step density, simply because the Pd adatom islands (see Fig. 4.5) require some time to disintegrate. Actually, the density difference leads to the introduction of vacancy islands when the surface is reduced, which contributes a small, abrupt increase to the step density. Continued cycles of oxidation and reduction further reduce the magnitude of these abrupt effects, but the trends stay for the roughness to decrease in the metal phase and increase in the oxide phase. Irrespective of these 'offsets' in step density introduced by the above, abrupt effects, we see that there is a one-to-one correspondence between the step density on the metal surface immediately prior to oxidation and the roughness on the surface oxide immediately after the transition and there is a similar one-to-one correspondence between the roughness on the surface oxide immediately prior to reduction and the step density on the metal surface immediately after the transition. It is evident that the effects described here will influence the energetics, but they will not change the qualitative picture. From the two roughnesses (metal and oxide), we show in Fig. 4.3 only that of the metal surface ($\mathrm{FWHM}_{\mathrm{metal}}$ at P^{*}_{CO}), just prior to the switching event. For simplicity we did not include these offsets in the numerical model.